Paper ID: 367

Numerical Simulation for Hydrodynamic Behavior of the Floating Platform of a Wind Turbine

Md. Shariar Badon[1], Mir Tareque Ali[2]
[1,2]Department of Naval Architecture & Marine Engineering, Bangladesh University of Engineering & Technology, Dhaka 1000, Bangladesh.
E-mail: 1812005@name.buet.ac.bd[1], mtarequeali@name.buet.ac.bd[2]

Abstract

Due to the rapid transition from fossil fuels to renewable energy sources, deep water floating offshore wind turbines (FOWTs) present a promising solution to harness abundant offshore wind resources. However, to ensure the structural stability and safe operation of these large-scale installations, a thorough evaluation of the hydrodynamic behaviour and motion characteristics of these structures are essential. In this study, numerical simulations in frequency domain are conducted for regular waves and in time domain for irregular wave conditions to analyze the hydrodynamic response of a moored DeepCwind semi-submersible FOWTs. For numerical simulations, ANSYS AQWA and Hydrostar, two commercial hydrodynamic software programs are used. The hydrodynamic radiation and diffraction problems in the frequency domain simulations are solved based on linear potential flow theory and some of the numerical results are validated against published results. The maximum surge response is obtained for head sea condition whereas heave response is not affected due to the change in wave heading angles. In the time domain simulations, a catenary mooring system comprising of three mooring lines are attached to the platform to model the coupled motion response of the semi-submersible FOWTs under realistic environmental condition. It is observed that the motion responses for surge, heave and pitch mode and the mooring lines tension increases with the increase in significant wave height.

Keywords: Floating offshore wind turbine (FOWT), ANSYS AQWA, Hydrodynamic response, Hydrostar, 3-D source distribution.

1. Introduction

Due to the rise of energy demand globally from renewable energy sources, wind energy stands an important renewable energy source that is growing rapidly as a sustainable power source. Wind power is considered as a cost-effective and viable solution to provide huge amount of clean energy in future. Onshore wind turbine farms are facing a number of limitations like lack of land availability, competing site uses, and environmental impacts. On the contrary, floating offshore wind turbines (FOWTs) can harness wind energy without facing these problems. Although the research on floating offshore wind turbine platforms began in the 1990s, the first prototype was built in 2007 [1]. Following this milestone achievement, rapid advancements were initiated in research, development for a variety of FOWT platform designs. Offshore turbines offer a number of benefits such as lower noise level, better wind quality with higher wind speeds. However, they face challenges like the need for advanced offshore wind farm technology, construction costs etc. [2]. FOWTs are generally categorized into three types: tension leg platforms (TLP), spar platforms, and semi-submersible platforms. Compared to spar-type and TLP wind turbines, semi-submersible wind turbines offer greater flexibility in varying seabed conditions and drafts, as well as significantly reduced installation costs due to simpler dockside assembly. The dynamic responses of various floating wind turbine systems have been studied by a number of researchers [3]. For instance, Zhang et al. [4] performed a comparative study of hydrodynamic performance among 3 FOWTs. Also Lin et al. [5] implemented hydrodynamic simulations of the semi-submersible Wind Float by examining mooring systems in irregular waves and exploring broken mooring lines scenarios. In the existing literature, mooring lines tensions and mooring lines breaking scenario for FOWT platforms are not widely focused. Therefore, in this study, the hydrodynamic performance of a catenary moored semi-submersible FOWT platform is investigated under realistic environmental condition. Two commercial hydrodynamic software programs, ANSYS AQWA and Hydrostar, are used. Some of the numerical results are validated against published results. Finally, motion responses and mooring lines

tensions including breaking scenarios are calculated for different wave heading angles as well as for various significant wave heights.

2. Mathematical Formulation

The motion response of a semi-submersible structure in the frequency domain can be formulated using potential flow theory and linear wave-body interaction principles. The body is subjected to small amplitude oscillations in water of uniform depth, induced by long-crested regular waves. Consider a three-dimensional body of arbitrary shape, freely floating in water, where the fluid is assumed to be incompressible, inviscid, and irrotational. We define a Cartesian coordinate system O-XYZ, with the OXY plane representing the undisturbed mean free water surface and the Z axis pointing vertically upwards. When the floating body is in its equilibrium position, the Z axis passes through the body's center of mass, as shown in Fig. 1. In regular waves, the linear potential Φ, which depends on both space and time, can be expressed as the product of a space-dependent term and a harmonic time-dependent term as follows:

$$\Phi(x,y,z;t) = Re[\phi(x,y,z).e^{-i\omega t}] \tag{1}$$

where $\phi(x,y,z)$ is time independent quantity and the potential function $\phi(x,y,z)$ can be separated into contributions from all modes of motion of the bodies and from the incident and diffracted wave fields as follows:

$$\phi = -i\omega[(\phi_0 + \phi_7)\zeta_a + \sum_{j=1}^{6}(X_j\phi_j)] \tag{2}$$

where ϕ_0 is the incident wave potential, ϕ_7 is the diffraction wave potential, ϕ_j represents potential due to motion of body in the jth mode i.e., radiation wave potential, X_j stands for the motion of body in jth mode and ζ_a is the incident wave amplitude. The incident wave potential can be expressed as:

$$\phi_0 = \frac{g}{\omega^2}\frac{\cosh[k(z+h)]}{\cosh kh}e^{ik(xcos\beta+ysin\beta)} \tag{3}$$

where β is the angle of incident wave relative to the positive x-axis, h is the depth of water, g is the gravitational acceleration and k is the wave number. Having the solved the velocity potentials, the pressure at any point on the structure can be determined from linearized Bernoulli's equation [6]:

$$p = -\rho\frac{\partial\Phi}{\partial t} = i\rho\omega\,\phi\,e^{-i\omega t} \tag{4}$$

Substituting Equation (2) into the Equation (4) we can write,

$$p = \rho\omega^2[(\phi_0 + \phi_7)\zeta_a + \sum_{j=1}^{6}(X_j\phi_j)]\,e^{-i\omega t} \tag{5}$$

Consequently, the wave exciting forces (F_k), the added mass coefficients (a_{kj}), and damping coefficients (b_{kj}), can be written respectively as follows:

$$F_k = -\rho\omega^2\zeta_a e^{-i\omega t}\int(\phi_0 + \phi_7).n_k.ds \tag{6}$$

$$a_{kj} = -Re\left[\rho\iint_s \phi_j.n_k.ds\right] \tag{7}$$

$$b_{kj} = -Im\left[\rho\omega\iint_s \phi_j.n_k.ds\right] \tag{8}$$

Upon solving the exciting forces, added mass coefficients, damping coefficients, the equations of six rigid body motions in the frequency domain can be written as: X_j

$$\sum_{j=1}^{6}(M_{kj} + a_{kj})\ddot{X}_j + b_{kj}\dot{X}_j + c_{kj}X_j = F_k \tag{9}$$

where $k = 1,2,\ldots.6$

where $M_{kj}, a_{kj}, b_{kj}, c_{kj}$ are the body inertia matrix, added mass coefficient matrix, damping matrix and hydrodynamic restoring matrix respectively in k^{th} mode due to motion in j^{th} mode, X_j is the vector containing translational and rotational oscillations about the co-ordinate axes and F_k is the wave exciting force matrix. The equation of motion in time domain can be written as:

$$\sum_{j=1}^{6}[(M_{kj}+m_{kj})\ddot{x}_j(t)+\int_{-\infty}^{t}K_{kj}\,(t-\tau)\dot{x}_j(\tau)d\tau+C_{kj}x_j(t)]=\ F_{wave,k}(t)+F_{moor,k}(t) \qquad (10)$$

where $k = 1,2,\ldots.6,\ M_{kj}$ is the inertia coefficient, m_{kj} is the frequency-independent added mass coefficient, K_{kj} is the retardation function, C_{kj} is the hydrostatic restoring force coefficient. $\ddot{x}$, $\dot{x}$ and x are the acceleration, velocity and displacement of the floating structure. $F_{wave,k}(t)$ is the wave exciting force, $F_{moor,k}(t)$ is the reaction force of the mooring lines.

3. The Numerical Model of The FOWT Platform

In this study, the OC4 DeepCwind semisubmersible [6] was chosen as the model for the Floating Offshore Wind Turbine (FOWT) platform. This platform consists of a primary column, which supports the wind turbine tower, and three offset columns. For simplicity, pontoons and braces are not included in the model, as shown in Fig.1. The principal dimensions and main characteristics of this model are defined in Table 1:

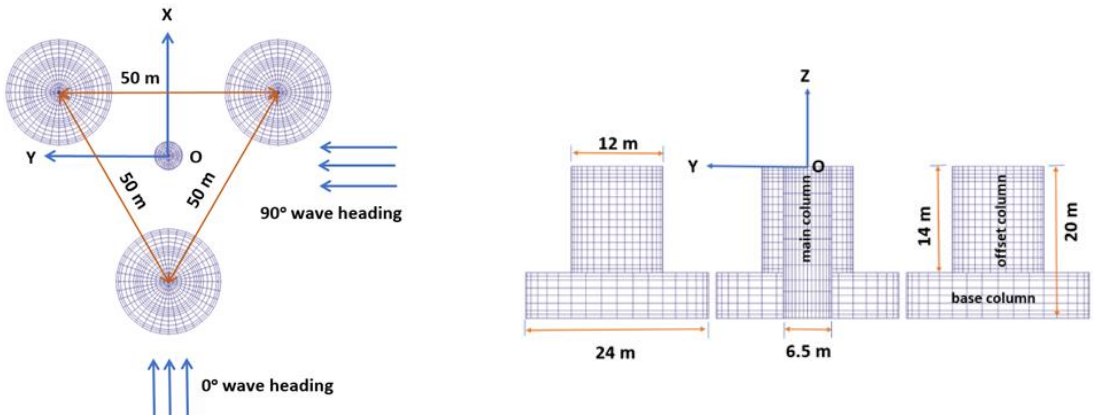


Fig. 1. Top and front view of the FOWT platform with circular base showing wave heading angles.

Table 1. The main dimensions and main characteristics of the platform

Parameters	Value
Depth of platform base below still water level (SWL)	20 m
Elevation of main column above SWL	10 m
Elevation of offset columns above SWL	12 m
Spacing between offset columns	50 m
Length of upper columns	26 m
Length of base columns	6 m
Diameter of main column	6.5 m
Diameter of offset columns	12 m
Diameter of base columns	24 m
Center of mass (CM) location below SWL	13.46 m
Platform roll and pitch inertia about CM	6.82E+9 kg-m^2
Platform yaw inertia about CM	1.22E+10 kg-m^2

To secure the platform, the OC4-DeepCwind semisubmersible is moored with three catenary lines spread symmetrically about the platform Z-axis. The mooring line properties are listed in Table 2

Table 2. Mooring system properties

Parameters	Value
Number of mooring lines	3
Angle between adjacent lines	120°
Depth to seabed below SWL	200 m
Unstretched mooring line length	835.5 m
Mooring line diameter	0.0766 m
Mooring lines extensional stiffness	753.6 MN

4. Results and Discussions

Figures 2(a) through 2(f) illustrate the frequency domain results of the added mass and damping coefficients for the surge, heave, and yaw modes. The numerical simulation results from ANSYS AQWA and Hydrostar are compared with the published results of Robertson et al. [6]. The figures show that the agreement between the numerical simulation results and the published results is quite satisfactory, except for the heave results, which show slight variations from the published data. These variations may be due to the omission of small diameter connecting members in the ANSYS AQWA and Hydrostar models. For the surge and yaw modes, the added mass coefficient remains constant at lower frequencies, but there is a sharp increase around 0.9 rad/s, and then again sharply decreases at higher frequencies. The damping coefficient is near zero at lower frequencies, with a sharp increase in magnitude around 1.1 rad/s, followed by a gradual decline. Whereas the heave added mass coefficients show minimal change with wave frequencies, as shown in Figure 2(c).

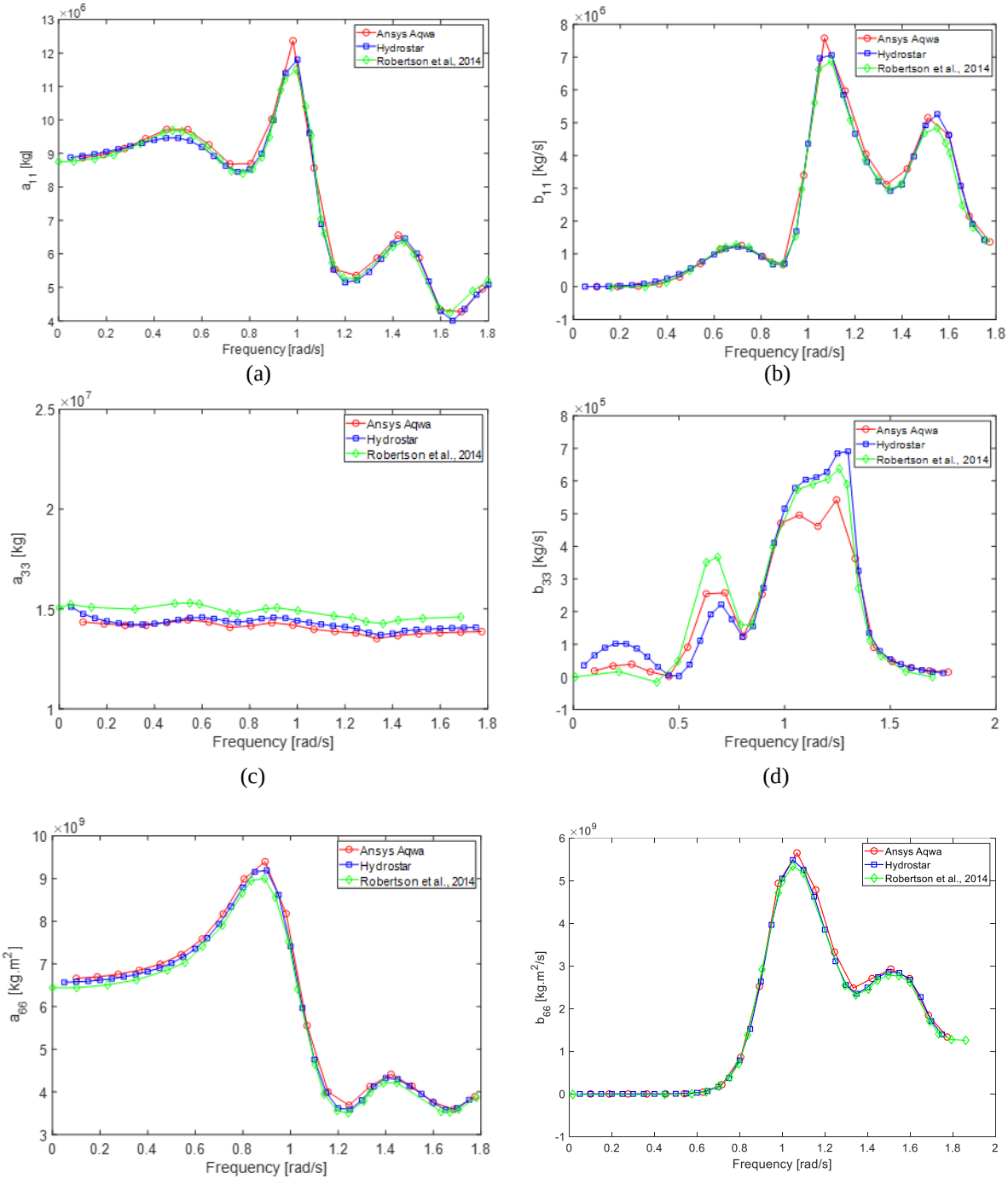


Fig. 2. Added mass and damping coefficients for surge, heave and yaw mode of the FOWT platform.

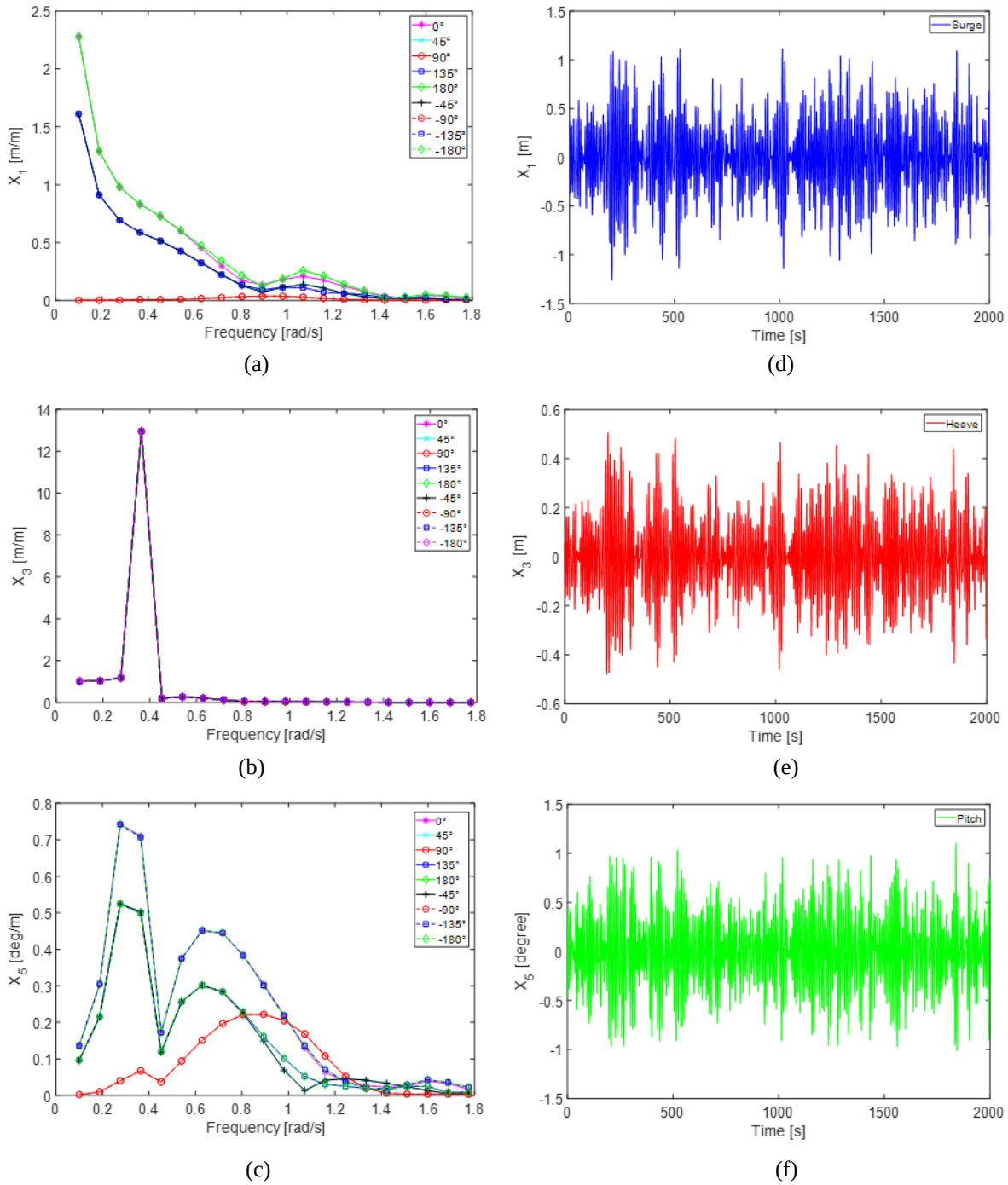


Fig. 3. Surge(X_1), heave(X_3) and pitch(X_5) motion responses of the FOWT platforms in frequency domain (a)~(c) for different wave headings and in time domain (d)~(f).

Figs. 3(a)~(c) show respectively the motion responses of surge, heave and pitch mode for different wave heading angles. The maximum surge motion is obtained for head sea (0^o *and* 180^o) and minimum for beam sea (45^o *and* 135^o). On the contrary, heave motion of the platform is not influenced by the wave heading angles. For pitch motion, different peak values are observed for different wave heading angles. Figs. 3(d)~(f) present time domain simulation results for a duration of 2000 sec, with a time step of 1 sec for surge, heave, and pitch mode. In Fig. 4 it is depicted that wave is heading along the mooring line 1, and it is 0 degree heading angle. Fig. 5(a) shows that as the significant wave height increases, the tension in cable 1 also increases due to its orientation with wave heading, while the tension in cable 2 and 3 as shown in Fig. 5(b) decreases. The tension in cable 2 and 3 is similar due to their similar orientation with the wave heading angle.

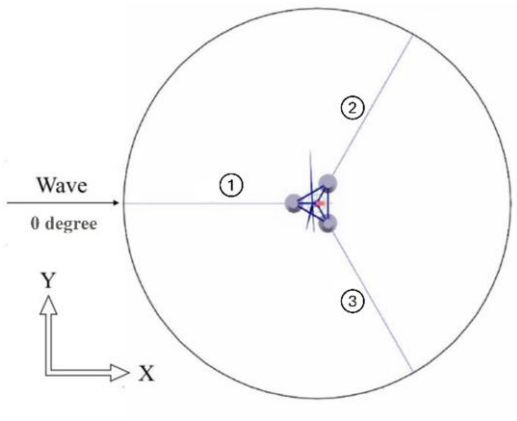
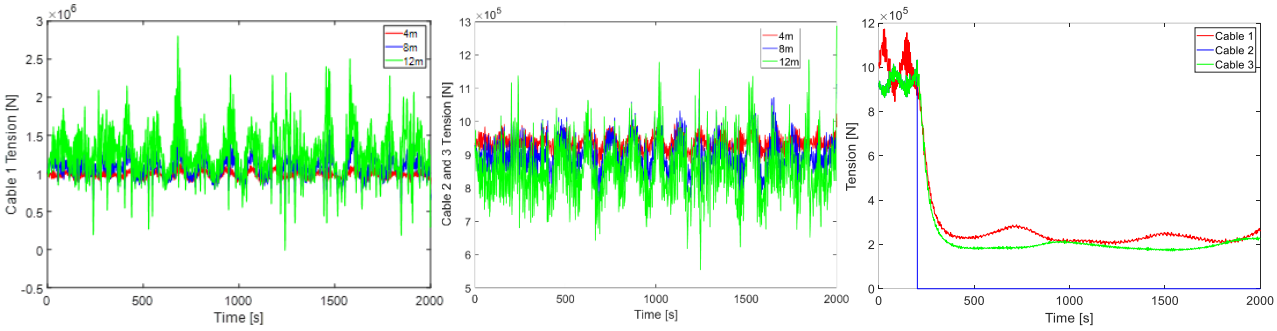


Fig. 4. Mooring line arrangement



(a) (b) (c)

Fig. 5. Mooring line tensions for different significant wave heights and for 0^o wave heading angle.

If cables 2 or 3 were to fail, when the wave is heading along 0 degree, most of the tension would shift to cable 1(as presented in Fig. 5(c)). Therefore, to prevent the mooring line failure, the stiffness of cable 1 is much important than the other two cables for the scenario considered in this study.

5. Conclusions

Numerical simulations were conducted to analyze the hydrodynamic response of moored DeepCwind semi-submersible FOWTs under both regular and irregular wave conditions. Two commercial hydrodynamic software programs, ANSYS AQWA and Hydrostar, were used for these simulations. For the time domain simulation, a catenary mooring system comprising of three mooring lines were attached to the platform and the mooring line breaking scenario was investigated. The maximum surge motion is obtained for head sea and minimum for beam sea. On the contrary, heave motion of the platform is not influenced by the wave heading angles. With the increase in significant wave height motion responses of the structure also increase. Heave response is less sensitive to the changes in wave heading angle compared to other modes. As wave height rises, tension increases in the cable aligned with the wave heading, whereas tensions decrease in the remaining cables.

6. References

[1] Edwards, E. C., Holcombe, A., Brown, S., Ransley, E., Hann, M . and Greaves, D, "Evolution of Floating Offshore Wind Platforms: A Review of at-Sea Devices," *Renewable and Sustainable Energy Reviews*,183, 2023.

[2] Esteban, M. D., Diez, J. J., López, J. S., and Negro, V., "Why offshore wind energy?" *Renew. Energy* 2011, 36, 444–450.

[3] Bachynski, E. E., and Eliassen, L., "The effects of coherent structures on the global response of floating offshore wind turbines," *Wind Energy*, 2018.

[4] Zhang, L., Shi, W., Karimirad, M., Michailides, C., and Jiang, Z., "Second-order hydrodynamic effects on the response of three semisubmersible floating offshore wind turbines," *Ocean Eng*. 2020, 207, 107371.

[5] Lin, Y. H., and Yang, C. H., "Hydrodynamic simulation of the semi-submersible wind float by investigating mooring systems in irregular waves," *Appl. Sci.* 2020, 10, 4267.

[6] Robertson, A., Jonkman, J., Masciola, M., Song, H., Goupee, A., Coulling, A., and Luan, C. "Definition of the Semisubmersible Floating System for Phase II of OC4", (National Renewable Energy Laboratory, NREL/TP-5000-60601, 2014)